RiESTech
Recent in Engineering Science and Technology

MBI

Article

Red Roselle (Hibiscus sabdariffa L.) Tea as an Organic Corrosion Inhibitor for Low-Carbon Steel in 3.5% Sodium Chloride Solution

Giafin Bibsy Rahmaulita [1,*], Johny Wahyuadi Mudaryoto Soedarsono [1]

[1] Department of Metallurgical and Materials Engineering, Universitas Indonesia, Depok, Indonesia 16424
* Correspondence: giafinbibsy@gmail.com

Abstract: Corrosion of low-carbon steel in chloride media remains a persistent challenge across infrastructure and multiple industrial sectors. This study evaluates red roselle (*Hibiscus sabdariffa*) tea as a green corrosion inhibitor for low-carbon steel in a 3.5wt% NaCl using weight-loss measurements over 3, 6, 9, and 12 days, complemented by pH and corrosion-potential observations. A red roselle-tea concentration of 10 g/L with an additional 2 mL of liquid inhibitor was employed. Relative to the uninhibited control, mass-loss data show a measurable reduction in corrosion, with inhibition efficiency increasing from 8% at day 3 to a maximum of 16% at day 9; no further improvement was observed at day 12. The tea also stabilized solution pH and shifted the corrosion-potential toward more noble (less negative) values, consistent with formation of an adsorbed, partially blocking film attributed to polyphenolic constituents. Observed efficiencies are modest and toward the low end of reported values for plant-based inhibitors in neutral 3.5 wt% NaCl, underscoring the need to optimize extract loading, extraction/fractionation strategy, and test conditions. The results provide a quantitative benchmark for advancing roselle-derived green inhibitors.

Keywords: Low-carbon steel; Green Corrosion Inhibitor; Red Roselle Tea; Sodium Chloride; weight-loss method

Citation:. Rahmaulita, G. B., Soedarsono, J. W. M. (2025). Red Roselle (Hibiscus sabdariffa L.) Tea as an Organic Corrosion Inhibitor for Low-Carbon Steel in 3.5% Sodium Chloride Solution. Recent in Engineering Science and Technology, 3(04), 24–35. Retrieved from https://www.mbi-journals.com/index.php/ riestech/article/view/119

Academic Editor: Vika Rizka

Received: 20 June 2025
Accepted: 19 October 2025
Published: 31 October 2025

1. Introduction

Corrosion is a natural and inevitable process that leads to the deterioration of metals as a result of their interaction with the surrounding environment, often resulting in adverse consequences [1]. In everyday life, corrosion is commonly observed in buildings, infrastructure, and tools that utilize metals such as low carbon steel as primary materials. The destructive effects of corrosion have significant implications, not only compromising structural integrity and safety but also impacting environmental sustainability and economic stability [2].

One effective approach to reducing the rate of corrosion involves the use of corrosion inhibitors—substances that, when introduced in small quantities into a corrosive environment, can significantly slow down the degradation of metals [3]. Inorganic inhibitors, though widely used, often consist of hazardous chemical compounds that are costly and environmentally unfriendly. In contrast, organic inhibitors, particularly those derived from plant-based sources, offer a more sustainable and eco-friendly alternative to conventional chemical inhibitors.

The use of plant extracts as corrosion inhibitors has gained increasing attention due to their widespread availability, lower cost, and environmentally friendly nature [4–5]. These so-called green inhibitors are typically derived from various plant components, including flowers,

seeds, leaves, stems, and roots. Numerous studies have demonstrated the effectiveness of natural extracts in reducing corrosion rates. For example, research conducted by Elachi [6] reported corrosion inhibition efficiencies of 27.95% and 22.81% when using leaf and flower extracts of roselle on mild steel in a 0.5 M tetraoxosulfate solution. The study highlighted that roselle extracts exhibit greater effectiveness during the first 8 days of exposure. Similarly, Ameer observed that the inhibition efficiency increases with higher concentrations of the extract, with experiments involving the addition of red roselle extract to hydrochloric acid (HCl) solutions. Further research demonstrated that roselle extract achieved an inhibition efficiency of up to 97.59% when applied to a copper–zinc (Cu–Zn) alloy in a 1 M nitric acid (HNO_3) solution [7-8]. These findings underscore the significant potential of roselle as a green corrosion inhibitor across various metals and corrosive environments.

Dried red roselle flowers are rich in bioactive compounds such as flavonoids, polyphenolic acids, anthocyanins, sabdaretin, and hibiscetin. The characteristic red coloration of roselle, commonly referred to as hibiscus pigment, has been attributed to compounds including delphinidin, delphinidin-3-monoglucoside, and cyanidin-3-monoglucoside [8]. These constituents are known for their antioxidant properties, which contribute to their potential role as corrosion inhibitors.

The objective of this study is to evaluate the effectiveness of red roselle tea as a corrosion inhibitor for low carbon steel in a 3.5% sodium chloride solution. The investigation is based on varying immersion times to assess inhibition performance. Due to its high antioxidant content, red roselle tea is anticipated to reduce the corrosion rate by forming a protective layer on the metal surface.

2. Materials and Experiment Methods

Immersion testing and post-exposure cleaning followed ASTM G31 and ASTM G1, respectively, to ensure reproducibility. Weight-loss measurements are complemented by pH tracking and corrosion-potential observations, with results reported from replicate trials. Figure 1 provides an overview of the experimental workflow to facilitate replication.

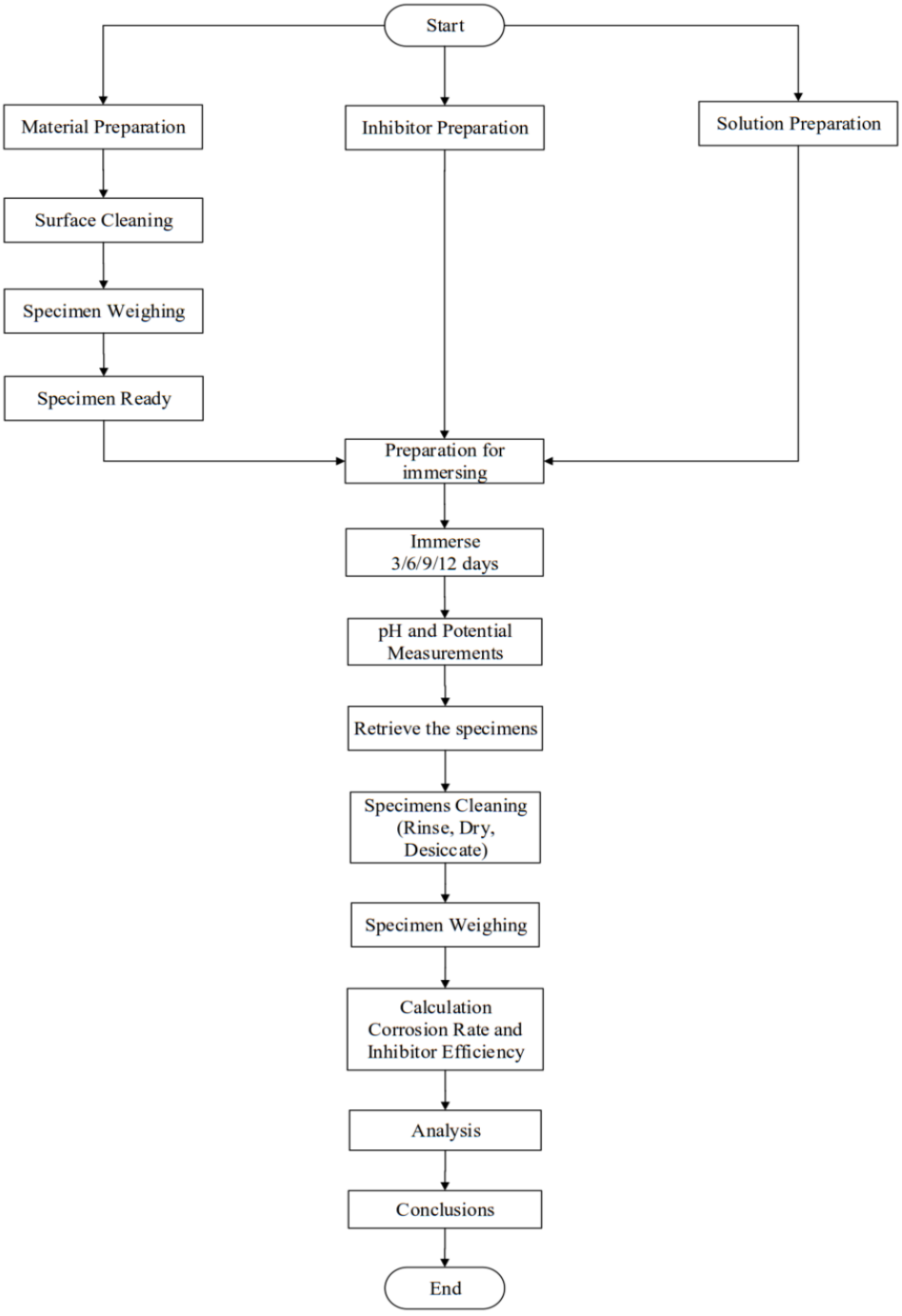

Figure 1. Experimental workflow integrating preparation, immersion, monitoring (pH, corrosion potential), post-exposure cleaning, and corrosion rate for low-carbon steel in 3.5 wt% NaCl.

2.1 Sample and Environment Preparation

The materials that will be used are low carbon steel. The sheets of low carbon steel are 1mm thick and cut into 24 sheets with measurements of 25mm x 20mm x 1mm. The top of the samples that have been cut are drilled into to create holes that each have a diameter of 3mm for the hanging of a sample in accordance with Figure 2. After, the sample was sanded starting with 80 grit to 240 grit sandpaper to remove oxides on the surface of the sample. Each sample was then weighed using a digital scale.

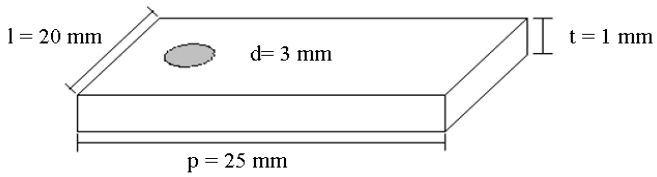

Figure 2. Illustrates the sample of the experiment

The solution that used is a solution of sodium chloride with a concentration of 3.5%, used as a simulation of sea water. To make the solution, dissolve 35 grams of Sodium chloride within 1 liter of distilled water. Based on ASTM G31-72, the volume of solution that can be found using the maximal ratio is 0.4 from the area of the surface of the sample.

Area of the surface of the sample:

$= (2 \times p \times l) + (2 \times p \times t) + (2 \times l \times t) - ((2\pi r^2) + (t \times 2\pi r))$

$= (2 \times 25 \times 20) + (2 \times 25 \times 1) + (2 \times 20 \times 1) - (2 \times 3{,}14 \times 1{,}52) + (1 \times 2 \times 3{,}14 \times 1{,}5)$

$= 1085{,}29\ mm^2$

Minimum volume = 0,4 x 1085,29 = 434,119 ml ≈ 450 ml

2.2 Inhibitor Preparation

The concentration of the inhibitor that will be used is 10 gpl. The method used will be inserting 1 gram of dry Rosela flowers into a glass beaker, then, adding 100 ml of distilled water, heating, then stirring with a magnetic stirrer to distill the flowers so that we produce a mixture of Rosela with a concentration of 10 gpl. strain the dregs out, wait until the mixture is cold then use the inhibitor as in Figure 3.

Figure 3. Roselle Tea as inhibitor

2.3 Soak Test

The prepared sample is then hanged with string then dipped into a plastic vessel that has been filled with the sodium chloride 3.5% solution ±450 ml at room temperature. Each sample is then dipped into 1 vessel. To ease the observation and research process, each vessel has been given a number and different treatment. The sample will be dipped into the solution of Sodium chloride without an inhibitor and with an addtional 2 ml added over 3, 6, 9 and 12 days.

After immersing the samples, each vessel had their metal potential measured. A multimeter was used to measure the metal potential, where each positive side is connected with the

sample and the negative side with standard electrodes Ag/AgCl. The final potential of each vessel was measured before raising the samples.

2.4 Calculations of Corrosion Rate and Inhibitor Efficiency

The corrosion rate in this study was determined using the mass loss method, which involves measuring the reduction in mass of the metal specimens due to corrosion. Initially, each sample was accurately weighed and subsequently immersed in the test solution for a specified duration. Upon completion of the immersion period, the samples were retrieved, cleaned to remove corrosion products, and reweighed. The difference between the initial and final weights represents the mass loss attributable to corrosion. This mass loss is then used to calculate the corrosion rate by considering the exposed surface area of the specimen, the duration of immersion, and the material density. The corrosion rate was computed using the standard formula, and the corresponding units and constants are presented in Table 1. The corrosion rate can be done with the following equation 1:

$$Corrosion\ Rate\ (MPY) = \frac{K.W}{D.A.T} \quad (1)$$

Where: K = constant (Table 2)
W = mass loss (gr)
D = mass type (gr/cm3)
A = surface area of immersed (cm2)
T = time (hours)

Table 1. Units of the corrosion rate with the constant K [1]

Corrosion Rate Units Desired	Constant (*K*) in Corrosion Rate Equation
mils per year (mpy)	3.45×10^6
inches per year (ipy)	3.45×10^3
inches per month (ipm)	2.87×10^2
millimetres per year (mm/y)	8.76×10^4
micrometres per year (um/y)	8.76×10^7
picometres per second (pm/s)	2.78×10^6
grams per square meter per hour (g/m^2·h)	$1.00 \times 10^4 \times D$
milligrams per square decimeter per day (mdd)	$2.40 \times 10^6 \times D$
micrograms per square meter per second (µg/m^2·s)	$2.78 \times 10^6 \times D$

The efficiency of the inhibitor shows that the percentage of the decline of corrosion rate with the addition of inhibitor can be compared with the corrosion rate without any additions to the inhibitor. The larger the efficiency of the enhibitor, the better the obstruction of the corrosion rate. Calculating the efficiency of the inhibitor using equation 2.

$$Inhibitor\ Efficiency = \frac{X_a - X_b}{X_a}\ x\ 100\% \quad (2)$$

Where: Xa = corrosion rate without inhibitor
Xb = corrosion rate with the addition of an inhibitor

3. Results and Discussion

3.1 Material Characterization Results

The sample has been tested at the Center for Material Processing and Failiure Analysis (CMPFA) using an Optical Emission Spectrometer. The results conclude that the composition of low carbon steel are as in Table 2. Based on the results in Table 2, the Optical Emission Spectroscopy (OES) analysis shows that the carbon steel used has a carbon content (C) of 0.057%, classifying it as low-carbon steel.

Table 2. Composition of the low carbon steel used

C (%)	Si (%)	S (%)	P (%)	Mn (%)	Ni (%)	Cr (%)
0.057	0.007	0.003	0.007	0.160	0.031	0.023
Mo (%)	**Ti (%)**	**Cu (%)**	**Nb (%)**	**V (%)**	**Pb (%)**	**Fe (%)**
<0.005[2]	<0.002[2]	0.121	<0.002[2]	<0.002[2]	<0.025[2]	Bal.

3.2 Visual Observation Results

Figures 4 and 5 illustrate the initial condition of the low carbon steel specimens prior to immersion in solutions with and without the added inhibitor. The surfaces originally exhibited a uniform gray oxide layer, covering the entire sample. To eliminate this oxidation and ensure a clean, reactive surface, the specimens were mechanically polished using a series of abrasive papers with grit sizes 80, 100, 150, and 240. This surface preparation was essential to standardize the initial condition of all samples before exposure to the test solutions.

a) **(b)** **(c)** **(d)**

Figure 4. Low-carbon steel coupons were assigned immersion durations are **(a)** 3, **(b)** 6, **(c)** 9, **(d)** 12 days in 3.5 wt% NaCl without inhibitor

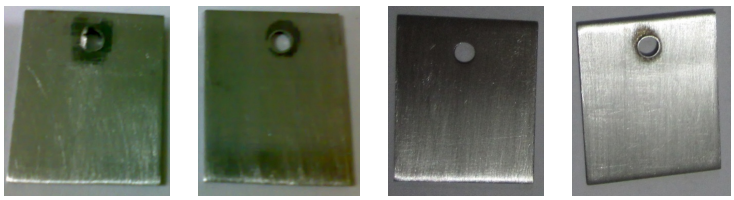

a) **(b)** **(c)** **(d)**

Figure 5. Specimen assignment for the roselle-inhibited condition **(a)** 3, **(b)** 6, **(c)** 9, **(d**) 12 days

After the immersion of 3, 6, 9, and 12 days, the sample which was submerged in the solution without an added inhibitor was raised and visually observed, the results can be seen in Figure 6. It can be seen that almost the entire surface of the sample has uniformly corroded. This uniform corrosion can be seen by the scale of yellow-reddish colors that has cover the

entire surface of the sample. The more time spent immersed, the more the scale will form. When pickled this scale can be cleaned easily but, it leaves marks and stains on the entirety of the surface of the metal which has been covered by the scale. The results of the visual observation after cleaning or pickling can be seen in Figure 7.

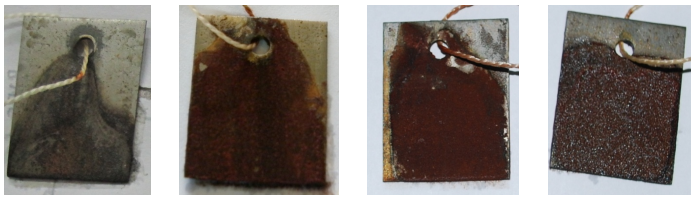

a) **(b)** **(c)** **(d)**

Figure 6. Uninhibited exposure, post-immersion appearance. Representative coupon surfaces after **(a)** 3, **(b)** 6, **(c)** 9, **(d)** and 12 days in 3.5 wt% NaCl, showing progressive accumulation of corrosion products

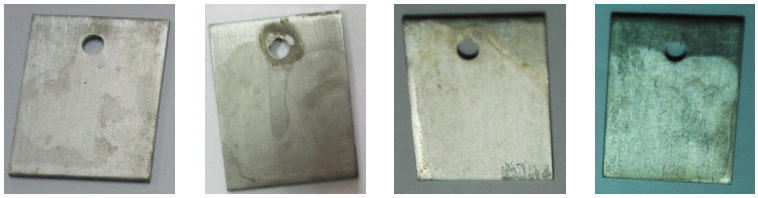

a) **(b)** **(c)** **(d)**

Figure 7. Uninhibited exposure, post cleaning surfaces. Representative coupons previously immersed for **(a)** 3, **(b)** 6, **(c)** 9, **(d)** 12 days in 3.5 wt% NaCl; images recorded after ASTM G1 cleaning reveal the underlying substrate following rust removal.

The sample with an added inhibitor's results can be seen in Figure 8. On the sample, the scale has a darker red coloration. But, the scale that covers the sample that was immersed in the solution with an added inhibitor has spread less and is not as thick when juxtaposed with the one without an added inhibitor. when pickled, the scale that has formed was more difficult to clean. Results of the visual observation after cleaning or pickling can be seen in Figure 9.

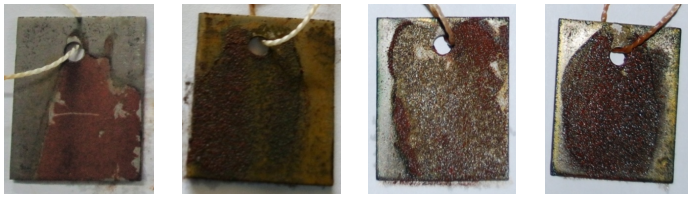

a) **(b)** **(c)** **(d)**

Figure 8. Inhibited, post-immersion surfaces. Representative coupons after **(a)** 3, **(b)** 6, **(c)** 9, **(d)** 12 days in 3.5 wt% NaCl, showing reduced corrosion-product coverage relative to the uninhibited

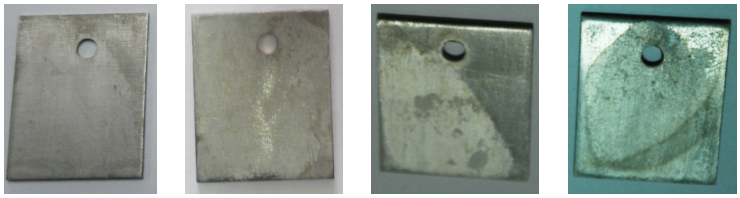

a) **(b)** **(c)** **(d)**

Figure 9. Inhibited, post-cleaning surfaces. Representative coupons previously immersed for **a)** 3, **(b)** 6, **(c)** 9, **(d)** 12 days in 3.5 wt% NaCl, images taken after ASTM G1 cleaning reveal the underlying substrate, indicating improved surface preservation relative to the uninhibited

3.2 Effects on pH and Corrosion Potential

The addition of the inhibitor led to an increase in the solution's alkalinity, suggesting that red roselle tea contributes to reducing the corrosiveness of the environment. This alteration indicates a stabilizing influence on the electrochemical conditions within the 3.5% sodium chloride solution. The observed pH differences between the inhibited and uninhibited systems are mainly attributed to the oxygen reduction reaction at cathodic sites. The pH change is illustrated in Figure 10a, representing the condition before immersion, and Figure 10b, reflecting the condition after immersion. The dominant cathodic reaction in such chloride-containing environments is expressed as:

$$\text{Oxygen reduction reaction:} \quad O_2 + 2H_2O + 4e \rightarrow 4OH^- \text{ [1]}$$

The oxygen reduction reaction results in the formation of hydroxide ions (OH^-), which contributes to an increase in the basicity of the environment. In systems containing organic inhibitors, such as red roselle extract, an oxygen scavenging mechanism is often observed. This mechanism reduces the availability of dissolved oxygen, thereby limiting the extent of the oxygen reduction reaction. As a consequence, the formation of OH^- is diminished, resulting in a more moderate increase in pH in the solution containing the inhibitor compared to the uninhibited system.

The measurement of corrosion potential showed a positive shift from –0.625 V to –0.572 V (vs. Ag/AgCl), indicating improved protection of the low carbon steel surface. Both the inhibited and uninhibited solutions were tested using a standard Ag/AgCl reference electrode. The potential changes are illustrated in Figure 11a, representing the condition prior to immersion, and Figure 11b, depicting the condition after the immersion period. The resulting potential values were averaged and then converted to the standard hydrogen electrode (SHE) scale using Equation (3):

$$Potential\ (V) vs\ SHE = potential\ (V) vs\ Ag/AgCl\ + 0{,}222V \qquad (3)$$

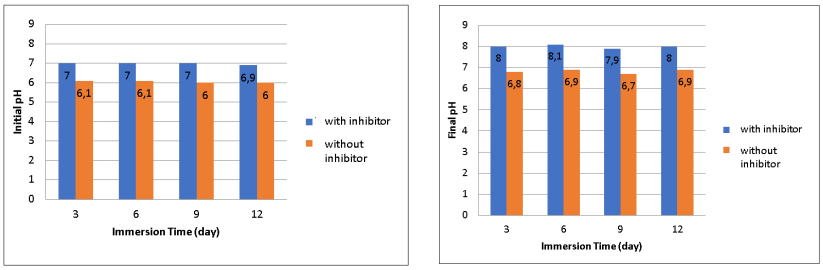

a) **(b)**

Figure 10. pH during immersion in 3.5 wt% NaCl. **(a)** Initial pH; **(b)** final pH at the end of each exposure (3, 6, 9, 12 d). Bars compare no inhibitor and roselle-inhibited conditions. The inhibited condition holds a higher, near-neutral to mildly alkaline than the unhibited, indicating pH stabilization consistent with inhibitor adsorption and weak buffering by the inhibitor

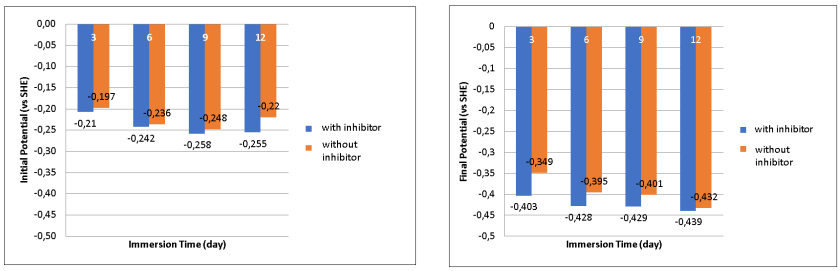

a) **(b)**

Figure 11. Corrosion potential during immersion in 3.5 wt% NaCl, reported vs SHE. **(a)** Initial; **(b)** final corrosion potential at the end of each exposure (3, 6, 9, 12 d). The inhibited condition shows a positive shift toward more noble potentials relative to the uninhibited.

3.3 Effects of Immersion Testing Period on the Weight Reduction of Metal, Corrosion Rate and Inhibitor Efficiency

Immersion tests at 3, 6, 9, and 12 days show clear time dependence: cumulative mass loss increases with exposure under both conditions but remains consistently lower when roselle tea is present, showed in Figure 12. Corrosion rates calculated from the weight-loss data follow this pattern. In the uninhibited condition, the rate evolves from 7.62 to 7.88 to 6.17 to 5.91 mpy (days 3→6→9→12), while the inhibited condition shows 7.02 to 6.68 to 5.17 to 5.19 mpy over the same interval. The minor rise at day 6 in the uninhibited condition and the slight uptick at day 12 in the inhibited case are typical early and late-stage transients superimposed on an overall downward trend. Inhibition efficiency mirrors this evolution, increasing from 7.93% (day 3) to 15.19% (day 6) and peaking at 16.08% (day 9) before easing to 12.28% (day 12), showed in Figure 13.

The time evolution of these metrics points to adsorption-controlled protection. At short times, a freshly prepared steel surface presents abundant active sites, so both anodic iron dissolution and the paired cathodic reaction proceed readily. As immersion continues, two coupled barriers develop at the interface. First, corrosion products accumulate and increase diffusion resistance to reactants. Second, organic constituents of the roselle tea adsorb on the

metal, occupying catalytic sites and forming a thin organic layer. The combined effect is a reduction of effective interfacial area and a slowdown of charge transfer, which explains the steady decrease in corrosion rate across the 12-day window and the consistently lower values in the inhibited condition.

The efficiency profile, rising through day 9 and moderating by day 12, further supports this mechanism. Early in exposure, surface coverage grows toward a compact, Langmuir-like monolayer as inhibitor molecules compete successfully for adsorption sites, yielding a marked improvement in protection, reflected in the increase from ~8% to ~16% efficiency between days 3 and 9. With longer exposure, partial desorption, rearrangement of the organic layer, or competitive penetration by chloride and dissolved oxygen can reduce the integrity of the protective film. In parallel, the corrosion-product layer may evolve toward a more porous or cracked morphology under sustained attack. Either pathway slightly diminishes the overall barrier, which is consistent with the modest loss of efficiency observed at day 12 alongside the small rate increase in the inhibited condition.

Apparent anomalies in the rate profile have a straightforward mechanistic basis. The day-6 rise in the uninhibited likely reflects the high reactivity of a freshly revealed steel surface together with a corrosion film that is still thin and discontinuous, as that film thickens and coalesces, the rate declines again by days 9 and 12. Likewise, the slight day-12 increase under inhibition is consistent with a modest shift in adsorption–desorption balance or the emergence of local defects within the mixed organic/corrosion-product layer, briefly exposing small areas of bare metal to the NaCl electrolyte.

In NaCl solution, the roselle tea suppresses metal dissolution across 3–12 days, with maximal effect at mid-exposure when the mixed organic/corrosion-product film is most compact and uniform. The modest late-stage attenuation is best attributed to interfacial reorganization partial desorption and the development of porosity rather than any change in the underlying electrochemical pathway. The convergent signatures time monotonic growth of mass loss, systematically lower corrosion rates in inhibited condition, and an efficiency profile that peaks before gently declining, are consistent with an adsorption-controlled inhibition mechanism for *Hibiscus sabdariffa* under the conditions studied.

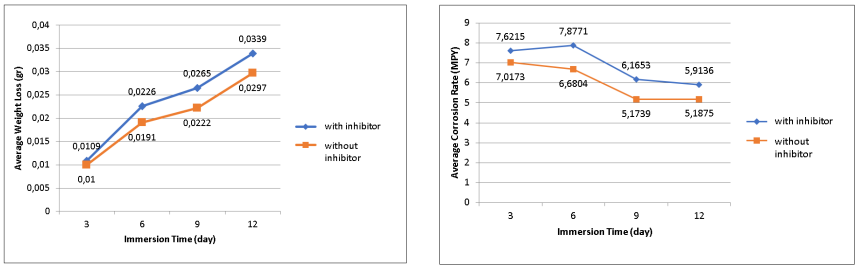

a) **(b)**

Figure 12. Mass loss **(a)** and corrosion rate **(b)**, versus immersion time (3, 6, 9, 12 d) in 3.5 wt% NaCl. Trends indicate progressive mass loss and a parallel decrease in CR; inhibition remains weak to moderate, maximizes near 9 days diminishing thereafter.

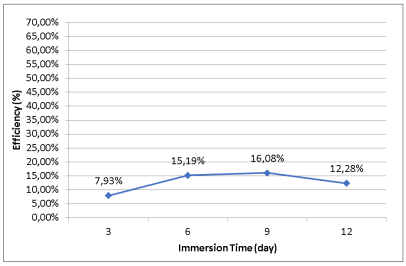

Figure 13. Weight loss based inhibition efficiency, η (%), versus immersion time in 3.5 wt% NaCl (roselle-inhibited condition). Efficiency rises from ~8% (3 days) to a maximum ~16% (9 days) and then declines to ~12% (12 days), indicating modest, time-dependent mitigation.

4. Conclusion

Roselle (*Hibiscus sabdariffa* L.) tea gives modest protection of low-carbon steel in 3.5 wt% NaCl. Weight-loss inhibition efficiency rises from ~8% (3 days) to ~15% (6 days), peaks near ~16% (9 days), then slips to ~12% (12 days). As expected, cumulative mass loss increases with time, while the instantaneous corrosion rate falls in both uninhibited and inhibited condition and stays lower with the extract. A slightly higher, more stable pH and a nobler potential under inhibition point to a partially blocking adsorbed/oxide film and a mixed-type inhibition behavior.

Performance and mechanistic clarity remain priorities. Subsequent studies should define the dose–response and persistence beyond 12 days; re-evalute the extraction by replacing brewed tea with a crude, non-thermal roselle flower extract that preserves thermolabile antioxidants (e.g., cold/hydroalcoholic extraction ≤40 °C); fractionate and quantify phenolics, correlating composition with inhibition efficiency (η); incorporate Tafel polarization to obtain $i_{(corr)}$ and resolve anodic/cathodic contributions; and verify film/rust chemistry via SEM/EDS, FTIR/ATR, and XRD. Sensitivity studies across temperature, pH, salinity, and hydrodynamics, together with benchmarking against a commercial green inhibitor under identical conditions, will define the practical operating window. Report replicate statistics (e.g., means with 95% confidence intervals) to convey effect size. These findings establish a quantitative baseline for advancing roselle-derived, environmentally benign inhibitors in chloride media.

Acknowledgments: The comments and suggestions from all the editors and reviewers are very much appreciated.

Conflicts of Interest: The authors declare no conflict of interest.

References

1. M. S. Sanders and E. J. Mccormick, *Human Factors in Engineering and Design*. McGraw-Hili, Inc., 1993. Fontana, G. 1986. *Corrosion Engineering*. New York: McGraw-Hill.
2. Asdim. 2008. "Penghambatan reaksi korosi baja dengan menggunakan ekstrak kulit buah manggis (*Garcinia mangostana* L.) sebagai inhibitor dalam larutan garam." Undergraduate thesis, Jurusan Kimia, Fakultas MIPA, Universitas Bengkulu.
3. Ilim, dan Beni Hermawan. 2008. "Studi penggunaan ekstrak buah lada (*Piper nigrum* Linn), buah pinang (*Areca catechu* Linn), dan daun teh (*Camellia sinensis* L. Kuntze) sebagai inhibitor korosi baja lunak dalam condition air laut buatan yang jenuh gas CO_2." Undergraduate thesis, Jurusan Kimia, FMIPA, Universitas Lampung.
4. Okafor, P. C., V. I. Osabor, and E. E. Ebenso. 2007. "Eco-friendly corrosion inhibitors: Inhibitive action of ethanol extracts of *Garcinia kola* for the corrosion of mild steel in H_2SO_4 solution." *Pigment and Resin Technology* 36: 299–305.
5. Rajendran, S., A. J. Amalray, M. J. Joice, N. Anthony, D. C. Trived, and M. Sundaravadivelu. 2004. "Corrosion inhibition by the caffeine-Zn system." *Corrosion Reviews* 22: 233–48.
6. Elachi, Emmanuel E., and Austine Justine. 2022. "Corrosion inhibition potentials of roselle (*Hibiscus sabdariffa*) in tetraoxosulphate(VI) acid solution." *International Journal of Engineering and Applied Physics* 2 (3).
7. Ameer. 2015. "Corrosion inhibition by naturally occurring *Hibiscus sabdariffa* plant extract on a mild steel alloy in HCl solution." *Turkish Journal of Chemistry*.
8. Seham, Shahen. 2022. "Eco-friendly roselle (*Hibiscus sabdariffa*) leaf extract as natural corrosion inhibitor for Cu–Zn alloy in 1 M HNO_3." *Egyptian Journal of Chemistry*.
9. Murthy, Z. V. P., and Vijayaragavan. 2021. "Mild steel corrosion inhibition by acid extract of leaves of *Hibiscus sabdariffa* as a green corrosion inhibitor and sorption behavior." *Green Chemistry Letters and Reviews*.
10. Okta, Malinda, dan Syakdani. 2021. "Pengujian berbagai aktivitas ekstrak air rosella secara *in vitro* (*Hibiscus sabdariffa* L.)." *Jurnal Kinetika* (Politeknik Negeri Sriwijaya).
11. Ahmed, A., and Al-Mashhadani. 2020. "Inhibition corrosion: Mechanisms and classifications—an overview." *Al-Qadisiyah Journal of Pure Science*.
12. Verma, Chandrabhan, and Akram Alfantazi. 2023. "Are extracts really green substitutes for traditional toxic corrosion inhibitors? Challenges beyond origin and availability." *Sustainable Chemistry and Pharmacy*.
13. Kaban, Agus Paul Setiawan, Wahyu Mayangsari, Mochammad Syaiful Anwar, Ahmad Maksum, Rini Riasutti, Taufik Adityawarman, and Johny Wahyuadi Soedarsono. 2022. "Experimental and modelling waste rice husk ash as a novel green corrosion inhibitor under acidic environment." *Materials Today: Proceedings* 62: 4225–34.
14. Soedarsono, Johny Wahyuadi, Muhammad Nafies Shihab, Muhammad Fikri Azmi, and Ahmad Maksum. 2018. "Study of *Curcuma xanthorrhiza* extract as green inhibitor for API 5L X42 steel in 1 M HCl solution." *IOP Conference Series: Earth and Environmental Science* 105 (1): 012060.